

Structural Characterization and Isotopic Abundance Ratios Analysis of Nanocurcumin Treated With Consciousness Energy Healing Treatment

Mahendra Kumar Trivedi¹ and Snehasis Jana^{2*}

¹Trivedi Global, Inc., Henderson, USA

²Trivedi Science Research Laboratory Pvt. Ltd., India

Article Information

Received date: Aug 19, 2019

Accepted date: Oct 19, 2019

Published date: Oct 21, 2019

*Corresponding author

Snehasis Jana, Trivedi Science Research Laboratory Pvt. Ltd., Thane (W), Maharashtra, India. Tel: 91-022-25811234; Email: publication@trivedieffect.com

Distributed under Creative Commons CC-BY 4.0

Keywords Nanocurcumin, The Trivedi Effect®; Energy of Consciousness Healing Treatment; LC-MS; GC-MS; Isotopic abundance ratio; Peak area%.

Article DOI 10.36876/smpmph.1029

Abstract

Nanocurcumin possesses diverse pharmacological effects, including anti-inflammatory, antioxidant, antiangiogenic activities, etc. The objective of the experiment was to investigate the impact of the Trivedi Effect®-Consciousness Energy Healing Treatment on the isotopic abundance ratios along with the structural properties of nanocurcumin using sophisticated spectroscopy techniques. Nanocurcumin powder was divided into two parts – one part of the sample was termed as control, while the other part was received the Trivedi Effect®-Consciousness Energy Healing Treatment by a famous Biofield Energy Healer, Mr. Mahendra Kumar Trivedi and termed as treated sample. The LC-ESI-MS analysis of both the control and treated nanocurcumin exhibited the protonated molecular ion mass at m/z 369 (calcd for $C_{21}H_{21}O_6^+$, 369.13) at retention time (R_t) 18.98 minutes along with similar fragmentation pattern. However, the relative peak intensities of the fragmented ion peaks of the treated nanocurcumin were significantly altered compared to the control sample. The isotopic abundance ratio of P_{M+1}/P_M ($^2H/^1H$ or $^{13}C/^12C$ or $^{17}O/^16O$) was significantly increased by 76.54% in the treated nanocurcumin compared to the control sample. Therefore, the ^{13}C , 2H , and ^{17}O contributions from $C_{21}H_{21}O_6^+$ to m/z 370 in the treated sample was significantly increased compared to the control sample. On the contrary, the isotopic abundance ratio of P_{M+2}/P_M ($^{18}O/^16O$) in the treated sample was significantly decreased by 28.39% compared to the control sample. Therefore, the ^{18}O contribution from $C_{21}H_{21}O_6^+$ to m/z 371 in the treated nanocurcumin was significantly decreased compared with the control sample. The GC-MS analysis showed that the chromatographic peak area% was significantly increased by 31.49% in the treated nanocurcumin compared to the control sample at R_t 10.68 minutes. The fragmented mass peak intensity of the treated sample at m/z 177 ($C_{10}H_9O_3^+$) and 192 ($C_{11}H_{12}O_4^+$) were significantly increased by 37.60% and 42.84%, respectively compared to the control sample. The proton and carbon signals for CH , CH_2 , OH , CO , COH , and OCH_3 groups in the 1H and ^{13}C NMR spectra of the treated and control samples were almost similar. The Trivedi Effect®-Consciousness Energy Healing Treatment might provide the necessary energy for the neutrino oscillations in nanocurcumin leads to the altered isotopic abundance ratio and improved solubility profile. Thus, the Biofield Energy Treated nanocurcumin would be more efficacious nutraceutical/pharmaceutical formulations for the treatment of inflammation, cancer, rheumatism, hyperglycemia, myocardial infarction, etc.

Introduction

Curcumin (diferuloylmethane) is a polyphenolic compound isolated from the dietary spice turmeric, i.e., rhizomes of Turmeric (*Curcuma longa* Linn) [1]. *Curcuma longa* rhizome contains linear diarylheptanoid, with molecules such as curcumin or derivatives of curcumin with different chemical groups called curcuminoids (2-6% of the rhizome). Curcuminoids contain 77% curcumin, 17% demethoxycurcumin, and 6% bisdemethoxycurcumin (Figure 1) [2,3]. Curcumin exhibits two tautomeric forms having a predominant keto form in neutral and acidic solutions, and stable enol form in alkaline medium [2]. Curcumin is the principal bioactive metabolite of *Curcuma longa*. From the ancient age, turmeric has been used for many ailments, particularly as an anti-inflammatory agent [2]. Curcumin tested as a potent antioxidant [4], besides it also shows the anti-inflammatory [5], antirheumatic [6], antimicrobial, antiproliferative [1], and anticancer [7] activities. Furthermore, curcumin is also well established for the hepato- and nephro-protective [8], myocardial infarction protective [9], thrombosis suppressing [10], and hypoglycemia [11].

In spite of broad the therapeutic effectiveness and promising therapeutic index, the curcumin is limited due to its poor absorption from the gastrointestinal tract (GIT) and poor bioavailability due to its rapid metabolism in the liver and intestinal wall [1,2]. Several kinds of the literature indicated that curcumin administered orally absorbed from the GIT, and present in the general blood circulation after being metabolized to the form of glucuronide and glucuronide/sulfate conjugates

OPEN ACCESS

ISSN: 2576-4004

[1,2,12,13]. Nanocurcumin is a modified form of curcumin where the particles of curcumin are transformed into nanoparticles that are practically more soluble and deliverable in the body. These curcumin nanoparticles have been shown to be more targeted to the tissue of interest that leads to better drug delivery and faster treatment without any wastage or side effects. To improve the bioavailability of curcumin, numerous approaches have been undertaken. Numerous published literature indicated that the Trivedi Effect®-Consciousness Energy Healing Treatment has the impact on the various properties of drug substances that would be helpful in the modification of physicochemical, spectral, and thermal properties of pharmaceutical/nutraceutical compounds [14-17]. Biofield Energy is a unique para-dimensional electromagnetic field exists in the human body, resulting in the continuous emission of energy from the body, which can freely flow between the human and environment [18,19]. Different religions, have recognized a living force that preserves and inhabits every living organism and believed to co-relate with the soul, spirit, and mind since from the ancient times. Scientifically, this hypothetical vital living force has been evaluated and is considered as Bioenergetics Field. There are several types of Biofield Energy Healing Therapies that are known for their significant positive impacts on various disease [20]. The Biofield Energy Healers have the ability to harness the energy from the “Universal Energy Field” and can transmit this energy into any living or non-living object(s), which respond to meaningful way, and the process is called Biofield Energy Healing Treatment. Such type of energy therapies are recommended by the National Institute of Health/National Center for Complementary and Alternative Medicine (NIH/NCCAM), and they included them under the Complementary and Alternative Medicine (CAM) due to their several advantages [21].

In recent years the Trivedi Effect®-Biofield Energy Treatment have been scientifically reported with remarkable and outstanding results in the field of biotechnology [22,23], microbiology [24,25], pharmaceutical/nutraceutical sciences [14-16], medical science [26,27], materials science [28,29], agriculture [30,31], etc. The Trivedi Effect® also found to have a remarkable effect of altering the isotopic abundance ratios of various compounds may be through the possible mediation of neutrinos [17,32,33]. Study on the natural stable isotope ratio analysis has wide applications in several fields of sciences to understand the isotope effects resulting from the alterations of the isotopic composition [34-36]. Gas chromatography-mass spectrometry (GC-MS) and liquid chromatography-mass spectrometry (LC-MS), are widely used for the analysis of isotope ratio with sufficient precision [35]. Therefore, in this experiment, the LC-MS based isotopic abundance ratio analysis of P_{M+1}/P_M ($^2\text{H}/^1\text{H}$ or $^{13}\text{C}/^{12}\text{C}$ or $^{17}\text{O}/^{16}\text{O}$) and P_{M+2}/P_M ($^{18}\text{O}/^{16}\text{O}$) samples was performed to evaluate the influence of the Trivedi Effect®-Consciousness Energy Healing Treatment on the isotopic abundance ratio in nanocurcumin. Consequently, the LC-MS, GC-MS, and NMR (Nuclear Magnetic Resonance) techniques were also used to characterize the structural properties of the nanocurcumin.

Materials and Methods

Chemicals and Reagents

The test sample nanocurcumin (40%) powder was purchased from Sanat Products Ltd., India, and other chemicals also used in the experiment were of analytical grade purchased in India.

Consciousness Energy Healing Treatment Strategies

The test sample nanocurcumin was equally divided into two parts. One part of nanocurcumin was termed as Biofield Energy Treated sample, which received the Consciousness Energy Healing Treatment by a famous Biofield Energy Healer, Mr. Mahendra Kumar Trivedi (USA) remotely under the standard laboratory conditions for 3 minutes. Besides, the other part of nanocurcumin was not received the Trivedi Effect®-Consciousness Energy Healing Treatment denoted as the control sample. But it was treated by a “sham” healer under the similar laboratory conditions, who did not have any knowledge about the Biofield Energy. Consequently, both the nanocurcumin samples were kept in similar sealed conditions and further analyzed by using sophisticated analytical techniques.

Characterization

Liquid Chromatography-Mass Spectrometry (LC-MS) Analysis and Calculation of Isotopic Abundance Ratio

The LC-MS analysis of both the nanocurcumin samples was carried out with the help of LC-Dionex Ultimate 3000, MS-TSQ Endura (USA) having a photo-diode array (PDA) detector connected with a Thermo Scientific TSQ Endura (USA) triple-stage quadrupole mass spectrometer with heated electrospray ionization (ESI) probe. The separation made in a reversed-phase Zorbax SB-C18 100 × 4.6mm × 3.5μm column (40°C). The mobile phase was 2mM ammonium formate and 0.5% formic acid in water and acetonitrile at a constant flow rate of 0.6 mL/min. The injection volume was 10μL, and the total run time was 35 min. Chromatographic separation was achieved using gradient condition as follow: 0 min-5% B, 5 min-5% B, 15 min-60% B, 20 min-95% B, 25 min-95% B, 30 min-5% B, and 35 min-5% B. The mass spectrometric analysis was performed under +ve ESI mode.

The natural abundance of the common elements C, O, and H are obtained from the literature [37-40]. The isotopic abundance ratios (P_{M+1}/P_M and P_{M+2}/P_M) for the control and Biofield Energy Treated nanocurcumin was calculated.

$$\% \text{ change in isotopic abundance ratio} = [(IAR_{\text{Treated}} - IAR_{\text{Control}}) / IAR_{\text{Control}}] \times 100]$$

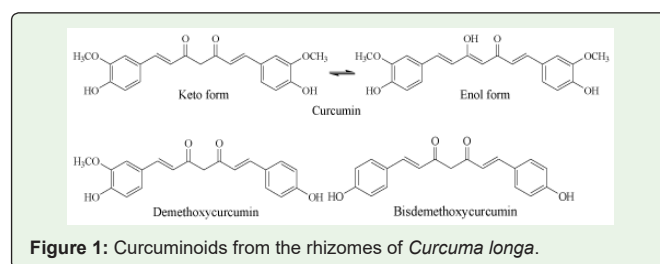


Figure 1: Curcuminoids from the rhizomes of *Curcuma longa*.

Table 1: LC-ESI-MS isotopic abundance ratio analysis of control and treated nanocurcumin.

Parameter	Control sample	Biofield Energy Treated sample
P_M at m/z 369 (%)	100	100
P_{M+1} at m/z 370 (%)	19.95	35.22
P_{M+1}/P_M	0.1995	0.3522
% Change of isotopic abundance ratio (P_{M+1}/P_M) compared to the control nanocurcumin		76.54
P_{M+2} at m/z 371 (%)	6.41	4.59
P_{M+2}/P_M	0.0641	0.0459
% Change of isotopic abundance ratio (P_{M+2}/P_M) compared to the control nanocurcumin		-28.39

P_M = the relative peak intensity of the parent molecular ion M^+ ; P_{M+1} = the relative peak intensity of the isotopic molecular ion $[M+1]^+$, P_{M+2} = the relative peak intensity of the isotopic molecular ion $[M+2]^+$, and M = mass of the parent curcumin molecule.

Table 2: GC-MS chromatographic and mass spectra analysis at R_t 10.68 minutes of the control and treated

Parameters	Control sample	Biofield Energy Treated sample	% Change
Peak area%	18.83	24.76	31.49
Mass peak intensity at m/z 177	40502.12	55730.65	37.60
Mass peak intensity at m/z 192	43361.76	61938.27	42.84

Table 3: ^1H and ^{13}C NMR spectroscopic data of the control and treated nanocurcumin. of the control and treated nanocurcumin.t

Position	^1H NMR δ (ppm)		^{13}C NMR δ (ppm)	
	Control	Treated	Control	Treated
1, 1'	br, s(9.64)	br, s(9.64)	--	--
2, 2'	s(3.84)	s(3.84)	55.69	55.68
3, 3'	--	--	149.34	149.34
4, 4'	--	--	147.99	147.97
5, 5'	s(7.32)	s(7.32)	111.33	111.32
6, 6'	--	--	126.32	126.31
7, 7'	d(7.15, J = 8)	d(7.15, J = 8)	123.12	123.12
8, 8'	d(6.82, J = 8)	d(6.82, J = 8)	115.69	115.68
9, 9'	d(7.54, J = 16)	d(7.55, J = 24)	140.69	140.69
10, 10'	d(6.72, J = 8)	d(6.72, J = 8)	121.08	121.07
11, 11'	--	--	183.20	183.19
12	s(6.05)	s(6.06)	100.82	100.80

br- broad, s- singlet, and d-doublet.

Where IAR = isotopic abundance ratio in control and treated nanocurcumin.

Gas Chromatography-Mass Spectrometry (GC-MS) Analysis

An Agilent 7890B Gas chromatograph equipped with a silica capillary column (30 m x 0.25mm) (HP-5 MS) and coupled to a quadrupole detector with pre-filter (5977B, USA) was operated with electron impact (EI) ionization in positive/negative mode at 70 eV was used for the analysis. The oven temperature was programmed from 50°C (1 min hold) to 300°C @ 20°C/min to 200°C (10 minutes hold). Temperatures of the injector, detector (FID), auxiliary, ion source, and quadrupole detector were 250,300,280,230, and 150°C.

Nanocurcumin was dissolved in methanol, and 1.0 μL was splitlessly injected with helium as a carrier gas with a flow rate of 1.5 mL/min.

Nuclear Magnetic Resonance (NMR) Analysis

^1H NMR spectra of nanocurcumin were recorded at 400 MHz on Agilent-MRDD2 FT-NMR. Chemical shifts (δ) were in parts per million (ppm) relative to the solvent's residual proton chemical shift $\{(\text{CD}_3)_2\text{SO}, \delta = 2.5\}$. Similarly, ^{13}C NMR spectra of nanocurcumin were measured at 100 MHz on Agilent-MRDD2 FT-NMR spectrometer at room temperature. Chemical shifts (δ) were in parts per million (ppm) relative to the solvent's residual carbon chemical shift $\{(\text{CD}_3)_2\text{SO}, \delta = 39.52\}$.

Results and Discussion

Liquid Chromatography-Mass Spectrometry (LC-MS) Analysis

The LC-MS chromatograms of both the nanocurcumin samples showed three sharp peaks (Figure 2) at the retention times (R_t) of 18.51, 18.74, and 18.98 minutes. The %peak area at R_t 18.51, 18.74, and 18.98 minutes was 4.56, 25.68, and 68.44 in control and 4.21, 25.90 and 68.52 in the Biofield Energy Treated sample, respectively. It indicated that the polarity of the Biofield Energy Treated sample remained close

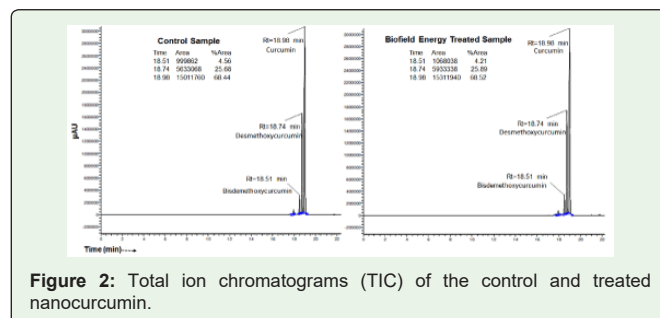


Figure 2: Total ion chromatograms (TIC) of the control and treated nanocurcumin.

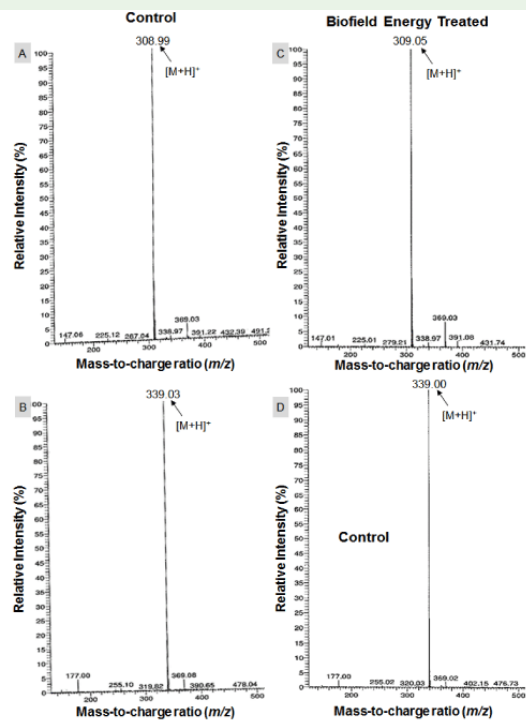


Figure 3: The ESI-MS spectra of the control (A and B) and treated (C and D)

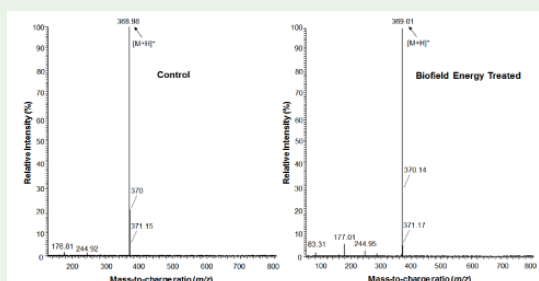


Figure 4: The ESI-MS spectra of the control and treated nanocurcumin at Rt 18.98 minutes in the chromatograms.

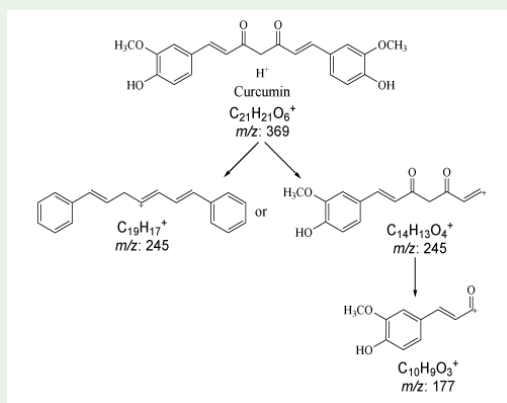


Figure 5: Proposed fragmentation pattern of control and treated nanocurcumin.

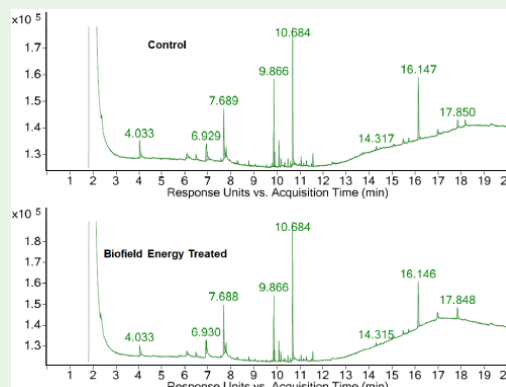


Figure 6: GC chromatograms of the control and treated nanocurcumin.

compared with the control nanocurcumin.

The ESI-MS spectra of the control and Biofield Energy Treated samples at R_t of 18.51 minutes exhibited the presence of the molecular mass of bisdemethoxy curcumin adduct with hydrogen ion (Figure 3) at m/z 309 (calcd for $C_{19}H_{16}O_4^+$, 309.11). Similarly, at R_t of 18.74 minutes showed the presence of the molecular mass of demethoxy curcumin adduct with hydrogen ion (Figure 3) at m/z 339 (calcd for $C_{20}H_{19}O_5^+$, 339.12). Curcuminoids are the molecules such as curcumin or derivatives of curcumin with different chemical groups that have been formed to increase the solubility of curcumin and make them suitable for drug formulation [1,2].

At the R_t of 18.98 minutes the corresponding molecular mass peak at m/z 369 (calcd for $C_{21}H_{21}O_6^+$, 369.13) was found to be curcumin adduct with hydrogen ion (Figures 4 and 5). Other lower mass peak at m/z 245 (calcd for $C_{14}H_{13}O_4^+$, 245.08 or $C_{19}H_{17}^+$, 245.08) and 177 (calcd for $C_{10}H_9O_3^+$, 177.05) in the control and Biofield Energy Treated samples were observed (Figures 4 and 5).

The ESI-MS spectra of the control and Biofield Energy Treated nanocurcumin showed almost similar type of mass fragmentation pattern (Figures 4 and 5). The molecular ion peak at m/z 369 exhibited 100% relative base peak intensity in both ESI-MS spectra (Figure 4). The relative peak intensities of the other ion peaks in the Trivedi Effect[®]-Consciousness Energy Healing Treated nanocurcumin were significantly altered compared to the control sample.

Isotopic Abundance Ratio Analysis

The control and Biofield Energy Treated samples of nanocurcumin showed the mass of a protonated molecular ion at m/z 369 ($C_{21}H_{21}O_6^+$) with 100% relative abundance in the mass spectra. The theoretical calculation of isotopic peak P_{M+1} for the protonated nanocurcumin presented as below:

$$P(^{13}C) = [(21 \times 1.1\%) \times 100\% \text{ (the actual size of the } M^+ \text{ peak)}] / 100\% = 23.1\%$$

$$P(^2H) = [(21 \times 0.015\%) \times 100\%] / 100\% = 0.315\%$$

$$P(^{17}O) = [(6 \times 0.04\%) \times 100\%] / 100\% = 0.24\%$$

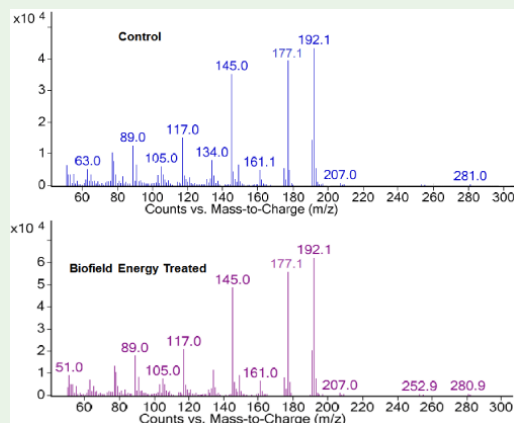


Figure 7: GC-MS spectra of the control and treated nanocurcumin at Rt 10.68 minutes.

P_{M+1} i. e. ^{13}C , ^2H , and ^{17}O contributions from $\text{C}_{21}\text{H}_{21}\text{O}_6^+$ to m/z 370 = 23.66%

Similarly, the theoretical calculation of isotopic peak P_{M+2} for the protonated nanocurcumin presented as below:

$$P(^{18}\text{O}) = [(6 \times 0.20\%) \times 100\%] / 100\% = 1.2\%$$

$$P_{M+2} \text{ of } ^{18}\text{O} \text{ contribution from } \text{C}_{21}\text{H}_{21}\text{O}_6^+ \text{ to } m/z \text{ 371} = 1.2\%$$

The calculated isotopic abundance of P_{M+1} value 23.66% was closer to the observed value (19.95%), but the calculated P_{M+2} value 1.2% was lower to the observed value (6.41%) (Table 1). Thus, the probability of $A + 1$ and $A + 2$ elements having an isotope with one and two mass unit heavier, respectively than the most abundant isotope (i.e., ^{13}C , ^2H , ^{17}O , and ^{18}O) contributions to the mass of the isotopic molecular ion $[M+1]^+$ and $[M+2]^+$. ^2H did not contribute much any isotopic m/z ratios because of its less natural abundance compared to the natural abundances of C and O isotopes [38,40]. From the calculations, it is confirmed that ^{13}C , ^{17}O , and ^{18}O have the major contributions from nanocurcumin to the isotopic mass peak at m/z 370 and 371. Therefore, P_M , P_{M+1} , and P_{M+2} of the nanocurcumin at m/z 369, 370, and 371 of the control and Biofield Energy Treated nanocurcumin were obtained from the experimental relative abundance of $[M]^+$, $[(M+1)^+]$, and $[M+2]^+$ peaks, respectively in the mass spectra (Table 1).

The isotopic abundance ratio of P_{M+1}/P_M ($^2\text{H}/^1\text{H}$ or $^{13}\text{C}/^{12}\text{C}$ or $^{17}\text{O}/^{16}\text{O}$) in the Trivedi Effect[®]-Consciousness Energy Healing Treated nanocurcumin was significantly increased by 76.54% compared to the control sample (Table 1). Thus, the ^{13}C , ^2H , and ^{17}O contributions from $\text{C}_{21}\text{H}_{21}\text{O}_6^+$ to m/z 370 in the Biofield Energy Treated sample was significantly increased compared to the control sample. On the contrary, the isotopic abundance ratio of P_{M+2}/P_M ($^{18}\text{O}/^{16}\text{O}$) in the Biofield Energy Treated nanocurcumin was significantly decreased by 28.39% compared to the control sample (Table 1). Therefore, the ^{18}O contribution from $\text{C}_{21}\text{H}_{21}\text{O}_6^+$ to m/z 371 in the Biofield Energy Treated nanocurcumin was significantly decreased compared with the control sample. Alteration in the number of neutrons in the molecule leads

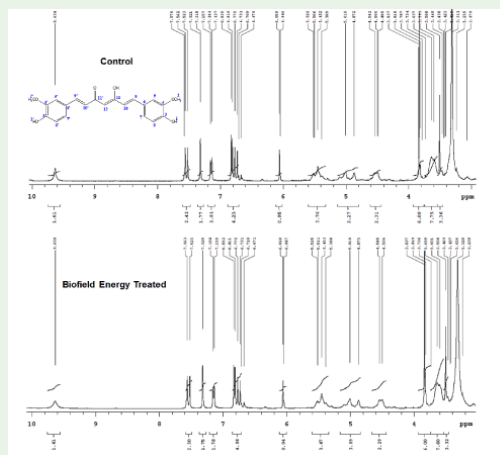


Figure 8: The ^1H NMR spectra of the control and treated nanocurcumin.

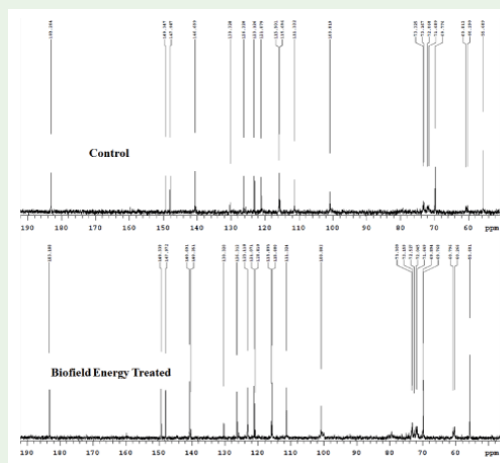


Figure 9: The ^{13}C NMR spectra of the control and treated nanocurcumin.

to the increased or decreased isotopic abundance of the compounds. Thus, it can be assumed that due to the possible mediation of neutrinos oscillation, the atomic mass and the atomic charge alter. Therefore, it is expected that the Trivedi Effect[®]-Consciousness Energy Healing Treatment might provide the necessary energy for the neutrino oscillations leads to the modification of the fundamental physicochemical properties of a compound [17,32,33]. The change in the kinetic isotope effects leads to the alteration in the isotopic abundance ratio of the atoms/molecules, which is very useful to study the reaction mechanism, understand the enzymatic transition state, and enzyme mechanism that is supportive for designing effective and specific inhibitors [32,33,35]. The treated nanocurcumin with altered isotopic abundance ratio (P_{M+1}/P_M and P_{M+2}/P_M) might be advantageous for the better nutraceutical/pharmaceutical formulations.

Gas Chromatography-Mass Spectrometry (GC-MS) Analysis

The chromatograms of both the control and Biofield Energy

Treated nanocurcumin showed several peaks (Figure 6) with very close retention time indicated that the polarity of the Biofield Energy Treated sample remained same compared with the control nanocurcumin. The mass spectra of both the control and Biofield Energy Treated samples (Figure 7) showed that m/z 177 (calcd for $C_{10}H_9O_3^+$, 177.05) and 192 (calcd for $C_{11}H_{12}O_3^{++}$, 192.08) are fragments of nanocurcumin, at R_t 10.68 minutes. The peak area% and mass peak intensities in the chromatograms and mass spectra, respectively of the Biofield Energy Treated nanocurcumin was significantly altered compared to the control sample (Table 2).

The chromatographic peak area% of the control and Biofield Treated nanocurcumin was 18.83 and 24.76, respectively (Table 2) at R_t 10.68 minutes. Therefore, the change in the peak area% was significantly increased by 31.49% in the Biofield Energy Treated nanocurcumin compared to the control sample. This indicated that the relative concentration of the nanocurcumin significantly increased compared to the control sample. The Trivedi Effect[®]-Consciousness Energy Healing Treatment might have influenced the physicochemical properties of nanocurcumin leads to an increase in the solubility and concentration in the solution. Increase in the solubility and concentration may improve the bioavailability of the nanocurcumin with desired (anticipated) pharmacological response [41].

The mass peak intensities of some major fragmented mass peaks were significantly altered (Table 2) at m/z 177 and 192. The mass peak intensity of the Biofield Energy Treated sample at m/z 177 (calcd for $C_{10}H_9O_3^+$, 177.05) was significantly increased by 37.60% compared to the control sample. Similarly, the mass peak intensity of the Biofield Energy Treated sample at m/z 192 (calcd for $C_{11}H_{12}O_3^{++}$, 192.08) was significantly increased by 42.84% compared to the control sample. The mass peak intensities were significantly increased may be due to the impact of the Trivedi Effect[®]-Consciousness Energy Healing Treatment. The Trivedi Effect[®] is a scientifically proved phenomena which have the remarkable potential to alter the isotopic abundance ratios of various compounds might be through the possible mediation of neutrinos [17,32,33].

Nuclear Magnetic Resonance (NMR) Spectroscopy Analysis

The 1H and ^{13}C NMR spectra are shown in Figure 8 and 9, respectively for the control and Biofield Energy Treated nanocurcumin. The 1H and ^{13}C NMR analyzed spectral data of both the control and Biofield Energy Treated nanocurcumin are presented in Table 3. The 1H NMR spectra of the control and Biofield Energy Treated samples (Figure 8) indicated that signals for the protons coupling of CH_2 , CH , OH , and OCH_3 protons of nanocurcumin were in the range of δ 3.84 to 9.64 ppm (Table 3), which were very close to each other. The experimental results were closely matched to the reported literature [42-44]. Similarly, the carbon signals for CH_2 , CH , COH , OCH_3 , and CO groups in the ^{13}C NMR spectrum (Figure 9) of the Biofield Energy Treated sample were almost same compared to the control sample of nanocurcumin (Table 3). The 1H and ^{13}C NMR results indicated that

there was no structural modification of the Biofield Energy Treated nanocurcumin compared to the control sample.

Conclusions

The Trivedi Effect[®]-Consciousness Energy Healing Treatment has shown the significant impact on nanocurcumin. The LC-ESI-MS analysis of both the control and Biofield Energy Treated nanocurcumin exhibited the protonated molecular ion mass at m/z 369 at R_t 18.98 minutes along with similar fragmentation pattern. However, the relative peak intensities of the fragmented ion peaks of the Biofield Energy Treated nanocurcumin were significantly altered compared to the control sample. The isotopic abundance ratio of P_{M+1}/P_M ($^2H/^1H$ or $^{13}C/^12C$ or $^{17}O/^16O$) was significantly increased by 76.54% in the Biofield Energy Treated nanocurcumin compared to the control sample. Therefore, the ^{13}C , 2H , and ^{17}O contributions from $C_{21}H_{21}O_6^+$ to m/z 370 in the Biofield Energy Treated sample was significantly increased compared to the control sample. On the contrary, the isotopic abundance ratio of P_{M+2}/P_M ($^{18}O/^16O$) in the Biofield Energy Treated sample was significantly decreased by 28.39% compared to the control sample. Therefore, the ^{18}O contribution from $C_{21}H_{21}O_6^+$ to m/z 371 in the Biofield Energy Treated nanocurcumin was significantly decreased compared with the control sample. The GC-MS analysis showed that the chromatographic peak area% was significantly increased by 31.49% in the Biofield Energy Treated nanocurcumin compared to the control sample at R_t 10.68 minutes. The fragmented mass peak intensity of the Biofield Energy Treated sample at m/z 177 ($C_{10}H_9O_3^+$) and 192 ($C_{11}H_{12}O_3^{++}$) were significantly increased by 37.60% and 42.84%, respectively compared to the control sample. From the results, it is concluded that the Trivedi Effect[®]-Consciousness Energy Healing Treatment might provide the necessary energy for the neutrino oscillations in nanocurcumin leads to the improvement of the therapeutic profile. The Trivedi Effect[®]-Consciousness Energy Healing Treatment could be an economical approach in the design of better nutraceutical and pharmaceutical formulations. Thus, the treated nanocurcumin with altered isotopic abundance ratio and improved solubility profile could provide better therapeutic response against inflammation, cancer, rheumatism, hypoglycemia, microbial infections, the hepato- and nephro-damage, myocardial infarction, thrombosis suppression, hypoglycemic condition, etc.

Acknowledgements

The authors are grateful to GVK Biosciences Pvt. Ltd., Trivedi Science, Trivedi Global, Inc., and Trivedi Master Wellness for their assistance and support during this work.

References

1. Anand P, Kunnumakkara AB, Newman RA, Aggarwal BB. Bioavailability of curcumin: Problems and promises. *Mol Pharmaceutics*. 2007; 4: 807-818.
2. Ravichandran R. Pharmacokinetic Study of Nanoparticulate Curcumin: Oral Formulation for Enhanced Bioavailability. *J Biomaterials Nanobiotechnology*. 2013; 4: 291-299.
3. Itokawa H, Shi Q, Akiyama T, Morris-Natschke SL, Lee KH. Recent advances in the investigation of curcuminoids. *Chinese Medicine*. 2008; 3:11.

4. Jayaprakasha GK, Rao LJ, Sakariah KK. Antioxidant activities of curcumin, demethoxycurcumin and bisdemethoxycurcumin. *Food Chemistry*. 2006; 98: 720-724.
5. Simal RC, Dhawan BN. Pharmacology of diferuloyl methane (curcumin), a non-steroidal anti-inflammatory agent. *J Pharmacy Pharmacol*. 1973; 25: 447-452.
6. Deodhar SD, Sethi R, Simal RC. Preliminary study on antirheumatic activity of curcumin (diferuloyl methane). *Indian J Med Res*. 1980; 71: 632-634.
7. Mahady GB, Pendland SL, Yun G, Lu ZZ. Turmeric (*Curcuma longa*) and curcumin inhibit the growth of *Helicobacter pylori*, a group 1 carcinogen. *Anticancer Res*. 2002; 22: 4179-4181.
8. Venkatesan N, Punithavathi D, Arumugam V. Curcumin prevents adriamycin nephrotoxicity in rats. *Br J Pharmacol*. 2000; 129: 231-234.
9. Nirmala C, Puvanakrishnan R. Protective role of curcumin against isoproterenol induced myocardial infarction in rats. *Mol Cell Biochem*. 1996; 159: 85-93.
10. Srivastava R, Dikshit M, Simal RC, Dhawan BN. Antithrombotic effect of Curcumin. *Thromb Res*. 1985; 40: 413-417.
11. Babu PS, Srinivasan K. Hypolipidemic action of curcumin, the active principle of turmeric (*Curcuma longa*) in streptozotocin induced diabetic rats. *Mol Cell Biochem*. 1997; 166: 169-175.
12. Qureshi S, Shah AH, Ageel AM. Toxicity studies on *Alpinia galanga* and *Curcuma longa*. *Planta Medica*. 1992; 58: 124-127.
13. Hsu CH, Cheng AL. Clinical Studies with Curcumin. *Adv Exp Med Biol*. 2007; 595: 471-480.
14. Trivedi MK, Patil S, Shettigar H, Bairwa K, Jana S. Spectroscopic characterization of chloramphenicol and tetracycline: An impact of biofield. *Pharm Anal Acta*. 2015; 6: 395.
15. Trivedi MK, Patil S, Shettigar H, Bairwa K, Jana S. Effect of biofield treatment on spectral properties of paracetamol and piroxicam. *Chem Sci J*. 2015; 6: 98.
16. Branton A, Jana S. Impact of consciousness energy healing treatment on the physicochemical and thermal properties of magnesium gluconate. *AJCE*. 2017; 5: 64-73.
17. Trivedi MK, Mohan TRR. Biofield Energy Signals, Energy Transmission and Neutrinos. *AJMP*. 2016; 5: 172-176.
18. Stenger VJ. Bioenergetic Fields. *The Scientific Review of Alternative Medicine*. 1999; 3.
19. Rogers M. Nursing: A Science of Unitary Human Beings. In J.P. Riehl-Sisca (ed.) *Conceptual Models for Nursing Practice*. 3rd Edn. Norwalk: Appleton & Lange. 1989.
20. Rubik B, Muehsam D, Hammerschlag R, Jain S. Biofield science and healing: history, terminology, and concepts. *Glob Adv Health Med*. 2015; 4: 8-14.
21. Barnes PM, Bloom B, Nahin RL. Complementary and alternative medicine use among adults and children: United States, 2007. *Natl Health Stat Report*. 2008; 12: 1-23.
22. Trivedi MK, Branton A, Trivedi D, Nayak G, Mondal SC, Jans S. Morphological characterization, quality, yield and DNA fingerprinting of biofield energy treated alphonso mango (*Mangifera indica* L.). *J Food Nutrition Sci*. 2015; 3: 245-250.
23. Trivedi MK, Branton A, Trivedi D, Nayak G, Mondal SC, Jans S. Evaluation of plant growth regulator, immunity and DNA fingerprinting of biofield energy treated mustard seeds (*Brassica juncea*). *Agriculture, Forestry and Fisheries*. 2015; 4: 269-274.
24. Trivedi MK, Branton A, Trivedi D, Nayak G, Mondal SC, Jans S. Antimicrobial sensitivity, biochemical characteristics and biotyping of *Staphylococcus saprophyticus*: An impact of biofield energy treatment. *J Women's Health Care*. 2015; 4: 271.
25. Trivedi MK, Branton A, Trivedi D, Nayak G, Shettigar H, Jans S. Antibiofilm of multidrug-resistant isolates of *Pseudomonas aeruginosa* after biofield treatment. *J Infect Dis Ther*. 2015; 3: 244.
26. Trivedi MK, Patil S, Shettigar H, Mondal SC, Jana S. The potential impact of biofield treatment on human brain tumor cells: A time-lapse video microscopy. *J Integr Oncol*. 2015; 4: 141.
27. Trivedi MK, Patil S, Shettigar H, Gangwar M, Jana S. In vitro evaluation of biofield treatment on cancer biomarkers involved in endometrial and prostate cancer cell lines. *J Cancer Sci Ther*. 2015; 7: 253-257.
28. Trivedi MK, Branton A, Trivedi D, Nayak G, Panda P, Jana S. Mass spectrometric analysis of isotopic abundance ratio in biofield energy treated thymol. *Frontiers in Applied Chemistry*. 2016; 1: 1-8.
29. Trivedi MK, Tallapragada RM. A transcendental to changing metal powder characteristics. *Metal Powder Report*. 2008; 63: 22-28.
30. Trivedi MK, Branton A, Trivedi D, Nayak G, Mondal SC, Jana S. Evaluation of plant growth, yield and yield attributes of biofield energy treated *Mustard (Brassica juncea)* and *Chick pea (Cicer Arietinum)* Seeds. *Agriculture, Forestry and Fisheries*. 2015; 4: 291-295.
31. Trivedi MK, Branton A, Trivedi D, Nayak G, Gangwar M, Jana S. Evaluation of Vegetative Growth Parameters in Biofield Treated *Bottle Gourd (Lagenaria siceraria)* and *Okra (Abelmoschus esculentus)*. *Int J Nutrition Food Sci*. 2015; 4: 688-694.
32. Trivedi MK, Branton A, Trivedi D, Nayak G, Panda P, Jana S. Evaluation of the isotopic abundance ratio in biofield energy treated resorcinol using gas chromatography-mass spectrometry technique. *Pharm Anal Acta*. 2016; 7: 481.
33. Trivedi MK, Branton A, Trivedi D, Nayak G, Panda P, Jana S. Gas chromatography-mass spectrometric analysis of isotopic abundance of ¹³C, ²H, and ¹⁸O in biofield energy treated p-tertiary butylphenol (PTBP). *AJCE*. 2016; 4: 78-86.
34. Schellekens RC, Stellaard F, Woerdenbag HJ, Frijlink HW, Kosterink JG. Applications of stable isotopes in clinical pharmacology. *Br J Clin Pharmacol*. 2011; 72: 879-897.
35. Muccio Z, Jackson GP. Isotope ratio mass spectrometry. *Analyst*. 2009; 134: 213-222.
36. Weisel CP, Park S, Pyo H, Mohan K, Witz G. Use of stable isotopically labeled benzene to evaluate environmental exposures. *J Expo Anal Environ Epidemiol*. 2003; 13: 393-402.
37. Rosman KJR, Taylor PDP. Isotopic compositions of the elements 1997 (Technical Report). *Pure Appl Chem*. 1988; 70: 217-235.
38. Smith RM. *Understanding Mass Spectra: A Basic Approach*, Second Edition, John Wiley & Sons, Inc, ISBN 0-471-42949-X. 2004.
39. Jürgen H. *Gross Mass Spectrometry: A Textbook* (2nd Edn) Springer: Berlin.
40. Meija J, Coplen TB, Berglund M, Brand WA, De Bièvre P, et al. Isotopic compositions of the elements 2013 (IUPAC technical report). *Pure Appl Chem*. 2016; 88: 293-306.
41. Savjani KT, Gajjar AK, Savjani JK. Drug solubility: Importance and enhancement techniques. *ISRN Pharm* 2012: 195727.
42. https://www.chemicalbook.com/SpectrumEN_458-37-7_1HNMR.htm.
43. https://www.chemicalbook.com/SpectrumEN_458-37-7_13CNMR.htm.
44. Koo HJ, Shin S, Choi JY, Lee KH, Kim BT, Choe YS. Introduction of methyl groups at C2 and C6 positions enhances the antiangiogenesis activity of curcumin. *Sci Rep*. 2015; 5: 14205.

Citation: Trivedi MK and Jana S. Structural Characterization and Isotopic Abundance Ratios Analysis of Nanocurcumin Treated With Consciousness Energy Healing Treatment. *SM Prev Med Public Health*. 2019; 3(1): 1029. <https://dx.doi.org/10.36876/smpmph.1029>